Skp2 Stabilizes Mcl-1 and Confers Radioresistance in Colorectal Cancer

Xinfang Yu
Central South University
Li Zhou
Central South University
Wenbin Liu
Hunan Cancer Hospital
lijun Liu
Central South University
Feng Gao
Central South University
Wei Li
Central South University
Haidan Liu (haidanliu@csu.edu.cn)
Clinical Center for Gene Diagnosis and Therapy https://orcid.org/0000-0002-6062-0813

Research

Keywords: Colorectal cancer, Irradiation, Skp2, Mcl-1, FBW7, Ubiquitination.

Posted Date: July 7th, 2021

DOI: https://doi.org/10.21203/rs.3.rs-645311/v1

Version of Record: A version of this preprint was published at Cell Death & Disease on March 1st, 2022. See the published version at https://doi.org/10.1038/s41419-022-04685-0.

Abstract

Background

Overexpression of Skp2 plays a critical role in tumorigenesis and correlates with poor prognosis in human malignancies. Thus, Skp2 has been proposed as an attractive target for anti-tumor interventions.

Methods

The expression of Skp2 in human colorectal cancer (CRC) and the role of Skp2 in tumorigenic properties and irradiation sensitivities of CRC cells were examined by anchorage-dependent and -independent growth assays, immunoblot, flow cytometry, immunohistochemical staining, ubiquitination analysis, co-immunoprecipitation assay, CRISPR-Cas9-based gene knockout, and xenograft experiments.

Results

Skp2 is highly expressed in CRC patient tissues. Blocking Skp2 expression reduces the tumorigenic properties of CRC cells *in vitro* and *in vivo*. Depletion of Skp2 confers sensitivity to irradiation of CRC cells. Skp2 deficiency enhances irradiation-induced intrinsic apoptosis by facilitating E3 ligase FBW7-mediated Mcl-1 ubiquitination and degradation. Knockout of Skp2 sensitizes CRC cells to irradiation treatments *in vivo*.

Conclusion

Our findings indicate that Skp2 stabilizes Mcl-1, and targeting Skp2 in combination with traditional radiotherapy might be efficacious in treating CRC.

Background

Colorectal cancer (CRC) ranks third for incidence and second for leading cause of cancer-related mortality worldwide(1). Curative-intent surgery combined with adjuvant radiotherapy is a mainstay of therapy for patients with CRC(2). Nevertheless, CRC patients face challenges related to treatment failure due to inherent and acquired radiation resistance. Novel agents target various genes, such as MEK, VEGF, PKC, HSP90, PARP, PD-1, PD-L1, and CTLA4, developed as radiosensitizers and conducted clinical trials in the treatment of colorectal cancer (2). To improve the effectiveness of radiotherapy for CRC, discovering potential targets to improve the radiosensitivity of CRC has important clinical significance.

Irradiation (IR) exerts its cytotoxic effects by inducing cell death, such as intrinsic apoptosis, which is regulated by the antiapoptotic and proapoptotic Bcl-2 family members. Disruption of the balance between antiapoptotic and proapoptotic Bcl-2 family members can change the cell fate from survival to

apoptosis. Myeloid cell leukemia 1 (Mcl-1) is an antiapoptotic Bcl-2 family member and is one of the most frequently overexpressed proteins in human cancers(3), including lung cancer (4), colorectal (5), liver (6), prostate cancer (7), and multiple myeloma (8). Mcl-1 inhibits cell death by binding to pro-apoptotic Bcl-2 family members to suppress mitochondrial outer membrane permeabilization and caspase activation, through which tumor cells evade the fate of death. Overexpression of Mcl-1 is an important reason for the resistance to various cancer therapies, including radio- and chemotherapies (9, 10). Moreover, several studies have demonstrated that downregulating Mcl-1 expression or reducing its stability are a benefit to the treatment of a variety of cancers (11–15). Therefore, Mcl-1 has emerged as an attractive target for therapeutic strategies.

In the present study, we found that depletion of Skp2 (S-phase kinase associated protein 2) enhances irradiation-induced apoptosis, which is accompanied by the decrease of the Mcl-1 protein level in human colorectal cancer cells. Targeting the Skp2-Mcl-1 axis is a promising anti-tumor strategy to overcome radioresistance in CRC.

Materials And Methods

Reagents and antibodies

Compounds, including MG132 and cycloheximide (CHX), were purchased from Selleck Chemicals (Houston, TX). Chemical reagents, including Tris, NaCl, SDS, and DMSO, for molecular biology and buffer preparation were purchased from Sigma-Aldrich (St. Louis, MO). Cell culture media and supplements were from Invitrogen (Grand Island, NY). Antibodies against Skp2 (#2652, IB:1:2000, IHC: 1:100), α-Tubulin (#2144, IB:1:10000), VDAC1 (#4866, IB:1:2000), Ubiquitin (#3936, IB: 1:1000), Mcl-1(#5453, IB: 1:1000), cytochrome C (#11940, IB:1:1000), Bax (#5023, IB: 1:1000), cleaved-caspase 3 (#9664, IB: 1:2000) and cleaved-PARP (#5625, IB: 1:2000) were obtained from Cell Signaling Technology, Inc. (Beverly, MA). Antibodies against β-actin (A5316, IB: 1:10000), Flag tag (F3165, IB: 1:10000), and Flag-HRP (A8592, IB: 1:20000) were from Sigma-Aldrich (St. Louis, MO). Antibodies against Ki67 (ab16667, IHC: 1: 250), FBW7 (ab109617, 1:1000), FBW7 (ab187815, 1:2000), donkey anti-rabbit IgG H&L (Alexa Fluor®568) (ab175470), and donkey anti-mouse IgG H&L (Alexa Fluor® 488) (ab150105) were purchased from Abcam (Cambridge, UK). Mcl-1(sc-819) for immunoprecipitate was from Santa Cruz (Dallas, TX). Secondary antibodies, including anti-rabbit IgG HRP (#7074) and anti-mouse IgG HRP (#7076), were purchased from Cell Signaling Technology. Antibody conjugates were visualized by chemiluminescence (ECL; cat#34076, Thermo Fisher Scientific).

Cell lines and cell culture

Human colorectal cancer cell lines HCT116 and HT29 were purchased from the American Type Culture Collection (ATCC, Manassas, VA). The 293T cell was purchased from ATCC and maintained in DMEM medium supplemented with 10% FBS and 1% antibiotics. All cells were maintained at 37°C in a

humidified incubator with 5% CO_2 according to the ATCC protocols. The cells were cytogenetically tested and authenticated before being frozen.

Immunohistochemical staining (IHC)

This study was approved by the Institute Research Ethics Committees of Xiangya Hospital, Central South University. Human colorectal cancer tissues and the paired adjacent tissues were obtained from the Department of Pathology at Xiangya Hospital with written informed consent (n=87). All the patients received no treatment before surgery. The tissues were fixed, embedded, and subjected to IHC analysis as described previously (13) . Briefly, after incubating at 65°C for 1 h, the tissue slides were submersed into sodium citrate buffer (10 mM, pH6.0) and boiled for 10 min, followed by incubation in 3% H_2O_2 for 10 min. Tissue slides were blocked with 50% goat serum albumin at room temperature for 1 h and incubated with the primary antibody in a humidified chamber overnight in a cold room. Tissue slides were washed with PBS and hybridized with the secondary antibody at room temperature for 45 min. Hematoxylin was used for counterstaining. Slides were viewed and photographed under a light microscope and analyzed using the Image-Pro Plus software (version 6.2) program (Media Cybernetics). The immunoreactions were evaluated independently by two pathologists as described previously (16) . Briefly, the percentage of positive cells was scored as follows: 0, no positive cells; 1, ≤10% positive cells; 2, 10-50% positive cells; 3, >50% positive cells. Staining intensity was scored as follows: 0, no staining; 1, weak staining; 2, moderate staining; 3, dark staining. Comprehensive score = staining percentage × intensity. Skp2 , Mcl-1 or FBW7 expression: ≤2 indicates low expression level; >2 indicates high expression level.

Transient transfection and generation of silencing stable cell lines

The generation of gene stable silencing cell line was performed as described previously (17) . Two different single-guide RNAs (sgRNAs) were used to generate CRISPR-Cas9-based Skp2 knockout constructs (sgSkp2#1 forward, 5’-AAGACTTTGTGATTGTCCGC-3’, reverse, 5’-CGGGACAATCA-CAAAGTCTT -3’; sgSkp2#2 forward, 5’-GCAACGTTGCTACTCAGGTC -3’, reverse, 5’-GACCTGAGTAGCAACGTTGC-3’). The Skp2 stable knockout signal clone was generated by transient transfection of sgSkp2 plasmids followed by selection with 1 mg/mL puromycin for 3 weeks. The Control siRNA (sc-37007), Mcl-1 siRNA (sc-35877), FBW7 siRNA (sc-37547) were purchased from Santa Cruz Biotechnology (Dallas, TX). Cells were grown in 6-well plates and transfected with 100 pmol small interfering RNA oligonucleotide using HiPerFect transfection reagent (Cat. 301705, Qiagen) for 72 h as described previously (18) . To confirm Mcl-1 or FBW7 knockdown, cells were harvested for protein extraction and immunoblotting.

Protein preparation and Western blotting

Whole-cell lysates were extracted with RIPA buffer (20 mM NAP, pH7.4, 150 mM NaCl, 1% Triton, 0.5% Sodium-deoxycholate, and 0.1% SDS) supplemented with protease inhibitors. Lysates were sonicated and centrifuged at 12,000 × g for 15 min. Protein concentration was determined using the BCA Assay Reagent (#23228, Pierce, Rockford, IL). Western blotting was performed as previously described (19) .

Cell viability assays

Cells were seeded at a density of 2×10^3 cells per well in 96-well plates in 100 μL of culture medium containing10% FBS and incubated in a 37 °C, 5% CO_2 incubator. Cells were treated with or without IR (2Gy). After culturing for another 24, 48, or 72 h, the MTS reagent (#G3581, Promega, Madison, WI) was added to each well, and cells were incubated for another 1 h at 37 °C and measured according to the standard procedures.

Anchorage-independent cell growth assay

Cells (8×10^3 per well) were treated with or without IR (2Gy) and seeded into six-well plates with 0.3% Basal Medium Eagle agar containing 10% FBS and cultured. The cultures were maintained at 37 °C in a 5% CO_2 incubator for 2 weeks, and colonies were counted under a microscope.

Plate colony formation assay

Cells were treated with or without IR (2Gy), and then seeded into the 6-cm plate (5×10^2/well). The cultures were maintained at 37 °C in a 5% CO_2 incubator for 2 weeks. The colonies were fixed with 4% paraformaldehyde and stained with 0.5% crystal violet. The numbers of the colony were counted under a microscope. Three independent experiments were performed in triplicate.

Trypan blue exclusion assay

The cell number and viability were assessed by counting the cells with a hemocytometer (Neubauer Chamber, Germany) using the trypan blue reagent, which distinguishes alive (bright) from dead cells or non-viable cells (blue ones).

Isolation of mitochondrial fractions

Cells from 10 cm plates were treated with or without IR (2Gy), harvested, and centrifuged at 850 × g for 2 min at 4 °C. The Mitochondria Isolation Kit (#89874, Thermo Fisher Scientific) was used for the extraction of the mitochondrial fractions according to the manufacturers' standard procedures.

Flow cytometry

Cells were treated with or without IR (2Gy) and seeded into six-well plates in culture medium containing 10% FBS. After treatment, attached and floating cells were harvested. For apoptosis analysis, the cells were suspended in 1×10^6 cells/mL, and 5 μL Annexin V and Propidium Iodide staining solution was added to 300 μL of the cell suspension. After incubated at room temperature for 15 min at dark, stained cells were assayed and quantified using a FACSort Flow Cytometer (BD, SanJose, CA, USA).

Ubiquitination assay

The ubiquitination assay was performed as described previously (16) . Briefly, cells were harvested and lysed with modified RIPA buffer (20 mM NAP, pH7.4, 150 mM NaCl, 1% Triton, 0.5% Sodium-deoxycholate, and 1% SDS) supplemented with protease inhibitors and 10 mM N-Ethylmaleimide (NEM). After sonication, the lysates were boiled at 95 °C for 15 min, and diluted with RIPA buffer containing 0.1% SDS, then centrifuged at 4 °C (16,000 × g for 15 min). The supernatant was isolated and incubated with specific antibody and protein A/G Sepharose beads overnight at 4 °C. After extensive washing, bound proteins were eluted with 2 × SDS sample loading buffer and separated on an SDS-PAGE, followed by Western blotting analysis.

In vivo tumor growth assay

The in vivo animal study was approved by the Institutional Animal Care and Use Committee (IACUC) of Central South University (Changsha, China). All mice were maintained and manipulated according to strict guidelines established by the Medical Research Animal Ethics Committee, Central South University, China. Cells (1×10^6) were s.c.injected into the 6-week-old athymic nude mice (n = 5) at the right flank to generate the xenograft mouse model. IR treatment was initiated when tumor volume reached at 100 mm^3. Mice were exposed to local ionizing radiation (2 Gy/ twice per week, irradiated with X-rays using X-RAD 320, Precision X-ray, Inc.,) and tumors were measured by caliper every 3 days. Tumor volume was recorded and calculated according to the following formula: tumor volume (mm^3) = (length × width × width/2). Mice were monitored until the endpoint. At that time, mice were euthanized and tumors extracted. Tumor mass was subjected to IHC staining.

Statistical analysis

Statistical analyses were performed using SPSS (version16.0 for Windows, SPSS Inc, Chicago, IL, USA) and GraphPad Prism 5 (GraphPad 5.0, San Diego, CA, USA). All quantitative data are expressed as mean ± s.e.m of three independent experiments. The difference between means was evaluated by the Student's *t*-test or ANOVA. Clinicopathologic significance in clinical samples was assessed by the χ^2 test or Fisher exact test for categorical data. Mann-Whitney *U*-test was used when the data did not fit a normal distribution. The Pearson rank correlation was used for correlation tests. Wilcoxon matched-pairs signed-rank test was used for evaluating the expression level difference between adjacent and tumor. A probability value of $p < 0.05$ was used as the criterion for statistical significance.

Results

Skp2 affects the tumorigenic properties and irradiation sensitivities of human colorectal cancer cells

To determine whether Skp2 is related to the tumorigenesis of human colorectal cancer, immunohistochemical (IHC) staining was performed to examine the protein level of Skp2 in colorectal cancer tissues. The results showed that Skp2 was upregulated in CRC tissues compared to the paired adjacent tissues (Fig. 1a). To investigate whether Skp2 affects the sensitivity of human CRC cells to irradiation (IR), we constructed Skp2 stable knockout HCT116 and HT29 cells. We found that depletion of

Skp2 (Fig. 1b) significantly decreased cell viability (Fig. 1c) and plate colony formation (Fig. 1d, e) in the presence of irradiation (2 Gy) in both HCT116 and HT29 cells. The anchorage-dependent colony formation potential of both Skp2-knockout HCT116 and HT29 cells in soft agar was impaired in the presence of irradiation (Fig. 1f, g). We next constructed a xenograft mouse model using HCT116-sgCtrl and HCT116-sgSkp2 stable cells. Xenograft tumors derived from Skp2-knockout HCT116 cells were treated with irradiation and exhibited a significant decrease in tumor growth, tumor mass, and tumor cell proliferation compared to tumors derived from Skp2-knockout cells that did not receive the irradiation or to tumors retaining Skp2 and treated with irradiation (Fig. 1h, i **and j)**. These results suggest that blocking Skp2 expression reduces the tumorigenic properties, and Skp2 deficiency confers sensitivity to irradiation of CRC cells.

Depletion of Skp2 enhances IR-induced apoptosis in human colorectal cancer cells

We next determined whether Skp2 deficiency affects irradiation-induced apoptosis of human CRC cells. The trypan blue exclusion assay showed that knockout of Skp2 decreased the population of live cells in the presence of irradiation in both HCT116 and HT29 cells (Fig. 2a). Pretreated with apoptosis inhibitor z-VAD-fmk partially recovered the population of live cells in the presence of irradiation (Fig. 2b), indicating that apoptosis is involved. By analyzing the activity of caspase 3, we showed that depletion of Skp2 increased the activity of caspase 3 in the presence of irradiation in both HCT116 and HT29 cells (Fig. 2c). Furthermore, the IB data demonstrated that IR-induced cleaved-caspase 3 and -PARP were up-regulated robustly in Skp2 knockout HCT116 and HT29 stable cells (Fig. 2d). The subcellular fractions, including mitochondrial and cytosolic fractions, were isolated to determine whether intrinsic apoptosis was involved. Irradiation decreased the expression of Bax in the cytosolic fraction but enhanced its protein level in the mitochondrial fraction of HCT116 cells (Fig. 2e). Consistently, the release of cytochrome c from mitochondria to the cytoplasm was increased with irradiation treatment (Fig. 2e). Knockout of Skp2 with irradiation treatment further promoted the protein level of cytochrome C in the cytosolic fraction, whereas the expression of cytochrome C in the mitochondrial fraction was reduced. Moreover, knockout of Skp2 with irradiation further increased the presence of Bax on mitochondria and decreased it in the cytoplasm (Fig. 2f) in HCT116 cells. Flow cytometry results indicated that knockout of Skp2 increased the apoptotic cells triggered by irradiation (Fig. 2g). These data suggest that depletion of Skp2 enhances irradiation-induced intrinsic apoptosis in human colorectal cancer cells.

Irradiation decreases Mcl-1 protein level in Skp2 deficient colorectal cancer cells

Our data showed that depletion of Skp2 downregulated Mcl-1 expression, and the protein level of Mcl-1 was further decreased when Skp2 depletion combined with irradiation treatment in both HCT116 and HT29 cells (Fig. 3a). Knockdown of Mcl-1 (Fig. 3b) and exposure to irradiation dramatically decreased the population of live cells (Fig. 3c), increased the activity of caspase 3 (Fig. 3d) in Mcl-1 silenced HCT116 and HT29 cells. We next determined whether overexpression of Mcl-1 compromised irradiation-induced apoptosis. The results revealed that ectopic overexpression of Mcl-1 (Fig. 3e) compromised irradiation decreased cell viability (Fig. 3f), anchorage-dependent **(Supplementary Fig. 1a)** and -independent colony

formation **(Supplementary Fig. 1b)**, as well as live cell population **(**Fig. 3g**)** in Skp2 depleted HCT116 and HT29 cells. Consistently, the activity of cleaved-caspase 3 was reduced with Mcl-1 transfection **(**Fig. 3h**)**. These data suggest that irradiation decreases the Mcl-1 protein level in Skp2 knockout cells is critical to irradiation-induced intrinsic apoptosis.

Irradiation Promotes Mcl-1 Ubiquitination And Degradation

To determine the mechanism of how irradiation downregulates Mcl-1 expression, we first performed qRT-PCR to analyze the transcription of Mcl-1 after Skp2 depletion with or without irradiation exposure. The result showed that the mRNA level of Mcl-1 was unaffected in Skp2 depleted CRC cells with or without irradiation treatment **(**Fig. 4a**)**, strongly suggesting that Mcl-1 is chiefly regulated by post-translational mechanisms. The Western blot results showed that Mcl-1 protein expression was blocked by Skp2 depletion and further decreased upon irradiation treatment in HCT116 and HT29 cells **(**Fig. 4b**)**. Notably, the proteasome inhibitor, MG132, restored Mcl-1 expression **(**Fig. 4b**)**. The ubiquitination analysis revealed that depletion of Skp2 increased Mcl-1 ubiquitination in HCT116 cells, indicating that Skp2 is required for Mcl-1 stabilization **(**Fig. 4c**)**. Moreover, Mcl-1 ubiquitination was increased by irradiation treatment, which was strongly promoted in Skp2 depleted HCT116 cells **(**Fig. 4d**)**. These data suggest that irradiation decreased Mcl-1 expression is related to protein degradation. Human Mcl-1 protein contains a total of 13 lysine residues, and five lysine residues, including K5, K40, K136, K194, and K197, have been shown to be ubiquitinated by FBW7 (20). To determine whether IR-induced Mcl-1 ubiquitination occurs on these lysine sites, we constructed a 5KR mutant, in which all of these five lysine residues were mutated to arginine. The *in vivo* ubiquitination result showed that IR-induced Mcl-1 ubiquitination was reduced markedly in the Mcl-1 5KR mutant in HCT116 cells **(**Fig. 4e**)**. IR decreased the protein level of Mcl-1 WT but not 5KR mutant in both HCT116 and HT29 cells **(**Fig. 4f**)**. Consistently, ectopic overexpression of Mcl-1 5KR rescued IR-decreased cell viability **(**Fig. 4g**)**, live cell population **(**Fig. 4h**)**, and colony formation **(**Fig. 4i**)**. These results suggest that irradiation promotes Mcl-1 ubiquitination and degradation, depletion of Skp2 enhanced irradiation-induced Mcl-1 destruction.

Fbw7 Is Required For Ir-induced Mcl-1 Ubiquitination

To determine how IR-induced Mcl-1 ubiquitination, we first examined the interaction between Mcl-1 and the E3 ligase FBW7. The result showed that FBW7 bound with Mcl-1 in HCT116 cells, and this interaction was elevated by the depletion of Skp2 **(**Fig. 5a**)**. Knockdown of FBW7 rescued Mcl-1 expression in Skp2-knockout HCT116 **(**Fig. 5b**)** and HT29 **(Supplementary Fig. 2a)** cells. Co-IP results demonstrated that irradiation (2Gy) significantly increased the interaction between Mcl-1 and FBW7 in HCT116 **(**Fig. 5c**)** and HT29 **(Supplementary Fig. 2b)** cells. Moreover, knockdown of FBW7 compromised irradiation-induced reduction of Mcl-1 and impaired IR-induced apoptosis in HCT116 **(**Fig. 5d**)** and HT29 **(Supplementary Fig. 2c)** cells. We further examined whether FBW7 regulates Mcl-1 ubiquitination. The result showed that suppression of FBW7 by small interfering RNA compromised Mcl-1 ubiquitination in Skp2 depletion cells

(Fig. 5e). Consistently, knockdown of FBW7 also decreased IR-induced Mcl-1 ubiquitination in HCT116 cells (Fig. 5f). To determine whether IR-induced Mcl-1 ubiquitination in Skp2-null cell is dependent on FBW7, we silenced FBW7 and examined Mcl-1 ubiquitination. The result showed that IR strongly induced Mcl-1 ubiquitination in Skp2-null HCT116 cells, and knockdown of FBW7 compromised this efficacy (Fig. 5g). Consistently, knockdown of FBW7 attenuated IR-decreased cell viability (Fig. 5h) and live cell population (Fig. 5i). Moreover, depletion of FBW7 decreased IR-induced caspase 3 activity (Fig. 5j) in Skp2-null HCT116 cells. These results suggest that FBW7 plays a critical role in IR-promoted Mcl-1 ubiquitination and destruction.

Irradiation Inhibits In Vivo Tumor Growth

We next investigated whether Mcl-1 affects the sensitivity of CRC cells to radiotherapy in *vivo*. We performed the xenograft tumors using HCT116 cells. Xenograft tumors derived from Mcl-1 knockdown HCT116 cells were treated with irradiation and exhibited a significant decrease in tumor growth (Fig. 6a), tumor mass (Fig. 6b), and tumor cell proliferation (Fig. 6c) compared to tumors derived from Mcl-1 knockdown cells that did not receive the irradiation treatment or to tumors retaining WT Mcl-1 and treated with irradiation (Fig. 6a). In the Mcl-1 knockdown HCT116 tumors, reintroduction of Mcl-1 5KR mutant impaired the anti-tumor effectiveness of irradiation treatment (Fig. 6a-c). We next determined the radiotherapeutic function of Mcl-1 ubiquitination *in vivo*. Xenograft tumors derived from Skp2-null HCT116 cells that were treated with irradiation exhibited reduced tumor growth (Fig. 6d), tumor mass (Fig. 6e), and tumor cell proliferation (Fig. 6f). However, silent of FBW7 in Skp2-null HCT116 cells rescues tumorigenesis under irradiation treatment (Fig. 6d-f). These results suggest that Mcl-1 stabilization confers radioresistance in CRC cells. Knockout of Skp2 sensitized CRC cells to radiotherapy is dependent on FBW7-mediated Mcl-1 ubiquitination and degradation.

Skp2 Positively Correlates With Mcl-1 In Crc Tissues

To determine the clinical relevance of our findings, we evaluated Skp2, Mcl-1, and FBW7 protein levels in 87 primary CRC specimens **(Supplementary Tables 1 and 2)** by immunohistochemical (IHC) analysis. The representative staining images with a high or low level of Skp2 expression, as well as Mcl-1 and FBW7, were shown (Fig. 7a). By systematically analyzing the IHC staining results, the details were summarized according to the score of Skp2, Mcl-1, and FWB7 (Fig. 7b-d). Among 87 patients, 38 cases of the high level of Mcl-1 were seen in all 53 individuals with a high level of Skp2 staining (Fig. 7e). In comparison, 39 of 49 patients with a high level of Mcl-1 exhibited downregulated protein level of FBW7 (Fig. 7f). Also, high Skp2 expression was accompanied by a low level of FBW7, 37 cases of the low level of FBW7 were detected in all 53 patients with a high level of Skp2 (Fig. 7g). As expected, a statistically significant positive correlation between Skp2 and Mcl-1 (Fig. 7h) and a negative correlation between FBW7 and Mcl-1 (Fig. 7i) were observed. These findings suggest that Skp2 positively correlates with Mcl-1, which is negatively correlated with E3 ligase FBW7, which may contribute to tumorigenesis of CRC.

Discussion

Mcl-1 is frequently overexpressed in various human tumors and contributes to tumor development, progression, and poor prognosis. Mcl-1 is a relatively short-lived protein and post-translationally regulated through ubiquitination and deubiquitination. E3 ubiquitin ligases, including Mule (21), β-TrCP (22) and FBW7 (13, 20, 23) have been identified to directly interact and induce Mcl-1 polyubiquitination and proteasomal degradation in response to apoptotic stimuli. E3 ligase Parkin has been implicated in Mcl-1 degradation in response to mitochondrial depolarization (24, 25). Trim17-mediated ubiquitination and degradation of Mcl-1 initiate apoptosis in neurons (26). FBXO4 is recently identified as an E3 ubiquitin ligase to interact and promote Mcl-1 ubiquitination and degradation in lung cancer (12). APC/C^{Cdc20} has been shown to engage in the ubiquitination of Mcl-1and to control Mcl-1 stability during mitosis (15, 27). Intriguingly, E3 ligase TRAF6 promotes nondegradative K63-linked polyubiquitination of Mcl-1 that antagonizes Mcl-1 interaction with the 20S proteasome, thereby protecting Mcl-1 from degradation elicited by chemotherapeutic drugs(28). The ubiquitylation can be reversed by deubiquitinases. Recently, deubiquitinase USP9X was described to stabilize Mcl-1 and promote tumor cell survival (29). Deubiquitinase Ku70 directly interacts with Mcl-1 to deubiquitinate and stabilize Mcl-1, leading to suppression of apoptosis (30). JOSD1 deubiquitinates and stabilizes Mcl-1 to suppress mitochondrial apoptotic signaling in gynecological cancer (31). DUB3/USP17L2 interacts with and deubiquitinates Mcl-1 in the cytoplasm of ovarian cancer cells, which protects Mcl-1 from degradation (32). USP13 is identified to act as a novel Mcl-1 deubiquitinase that enhances Mcl-1 stability and promotes tumor survival (33). Since the regulation of Mcl-1 stabilization depends on different stimuli and cell types, the identification of E3 ligases and DUBs that regulate Mcl-1 is important for Mcl-1-targeted therapies.

The Skp1-Cullin1-F-box protein (SCF) ubiquitin ligase complex is one of six mammalian cullin RING ubiquitin ligases (CRLs). The F-box protein subunit recognizes and binds the SCF substrates unusually in a phosphorylation-dependent manner. So far, at least six F-box proteins, including β-TrCP1, β-TrCP2, Skp2, FBW7, FBXL3, FBXL20, FBXO7, and FBXW8, have well-established and matched with their respective substrates (34). Skp2 and FBW7 are two different recognition subunits of the SCF E3 ligase complex that recognize specific substrates for ubiquitination.

Skp2 functions as an oncoprotein and exerts oncogenic functions through ubiquitination of its substrates such as p21 (35), p27 (36), p57 (37), E-cadherin (38), FOXO1 (39), Akt (40) and others. Therefore, Skp2 plays a crucial role in governing many key cellular processes, including cell growth, apoptosis, differentiation, cell cycle progression, migration, invasion, and metastasis (41). Skp2 is frequently overexpressed in a variety of human cancer (41, 42), including colorectal cancer (17). Moreover, overexpression of Skp2 is positively correlated with TNM stage, node capsular invasion, lymphovascular invasion and strongly associated with poor prognosis in CRC patients (43, 44). Additionally, Skp2 has been reportedly involved in the development of drug resistance (45–47) or radiation resistance (48). However, the role of Skp2 in CRC radiation resistance remains unclear.

FBW7 functions as a tumor suppressor and is commonly downregulated in cancer. Aberration or inactivation of FBW7 expression has been observed in human cancers, such as breast cancer (49), and leukemia (50), which is thought to be involved in tumorigenesis, progress, prognosis and drug resistance (23, 51, 52). FBXW7 mRNA expression is reported to be significantly reduced in colorectal cancer (20, 53, 54). FBW7 targets many well-characterized oncoproteins, including c-MYC (55), CyclinE (56), c-JUN (57), Mcl-1 (23), and Notch intracellular domain 1 (NICD1) (58) for ubiquitylation-mediated proteasomal degradation (51). Intriguingly, the stability and proteasomal degradation of FBW7 itself is regulated by deubiquitinase USP9X (59) and E3 ligase TRIP12 (60). Our results showed a trend that Skp2 is required for maintaining of Mcl-1 stability in IR treated CRC cells. Depletion of Skp2 enhanced IR-induced Mcl-1 ubiquitination, which was dependent on the E3 ligase FBW7.

An increasing number of pharmacological agents target for inhibiting E3 ligases and deubiquitinases have been developed. The MDM2 inhibitor Nutlin-3 effectively restores p53 function and induces cell cycle arrest and apoptosis in MDM2 expression human rhabdomyosarcoma cells with wild-type p53 (61). Serdemetan, an MDM2 inhibitor, mitigates experimental pulmonary hypertension (PH) in mice, partially through the inhibition of MDM2-mediated ubiquitination of angiotensin-converting enzyme 2 (ACE2) and thus rectified ACE2 expression (62). APC/C^{cdc20} inhibitor Apcin suppresses the metastasis in triple-negative breast cancer (63). Skp2 inhibitor SZL P1-41 restricts cancer stem cell traits and cancer progression by selectively suppressing Skp2 ubiquitin ligase activity (64). USP14 inhibitor IU1 significantly increases CD36 ubiquitination and stabilizes CD36 protein via removing the polyubiquitin chains, which result in the decreases of foam cell formation by downregulating CD36-mediated lipid uptake and provides a potential therapeutic target for atherosclerosis (65). Spautin-1 reportedly suppresses autophagy by inhibiting the USP10 and USP13 deubiquitinases (66). P22077, a dual inhibitor of USP7/USP47 (67), overcomes tyrosine kinase inhibitor resistance and eradicates leukemia stem/progenitor cells in chronic myelogenous leukemia through inhibits its novel substrate Y-box binding protein 1 (YB-1) deubiquitination and suppresses DNA damage repair (68). Several pharmacological agents have been shown to diminish Mcl-1 expression by inhibiting Mcl-1 production or enhancing Mcl-1 degradation. For instance, the USP9X inhibitor WP1130 lowers Mcl-1 levels in chronic myelogenous leukemia and enhances sensitivity to apoptosis by facilitating Mcl-1 degradation (69). Thus, further discovery of highly selective and effective E3 ligases and deubiquitinases inhibitors with fewer side effects are required for clinical treatment.

Conclusion

Targeting Mcl-1 appears to be a promising strategy in cancer therapy. Unfortunately, there were no Mcl-1 inhibitors have been approved currently. Our results indicated that irradiation induces CRC cell apoptosis through FWB7-mediated Mcl-1 degradation. Mcl-1 is involved in the regulation of radiosensitivity of CRC cells and might be a target for CRC radiosensitization. The combination of E3 ligases upstream of Mcl-1 with traditional radiotherapy would be efficacious in treating CRC.

Abbreviations

CRC
Colorectal cancer, IB:Immunoblotting; IHC:Immunohistochemical staining; CHX:cycloheximide; Cyto:cytoplasmic fraction; Mito:Mitochondrial fraction; IR:Irradiation; Mcl-1:Myeloid cell leukemia 1; sgRNAs:single-guide RNAs.

Declarations

Ethics approval and consent to participate

The animal experiments were approved by the Medical Research Animal Ethics Committee, Central South University, China.

Consent for publication

Not applicable.

Availability of data and materials

Materials are available upon request.

Competing interests

The authors have declared no conflicts of interest.

Funding

This work was supported by the National Natural Science Foundation of China (No. 82073260, 81972837, 82003203).

Author's contributions

Conception and design: F. Gao, W. Li, X.-F Yu, H.-D Liu; Development of methodology: F. Gao, W. Li, L. Zhou, W.-B Liu, L.-J Liu, X.-F Yu, H.-D Liu; Acquisition of data: X.-F Yu, F. Gao, W. Li, L. Zhou, W.-B Liu, L.-J Liu, H.-D Liu; Analysis and interpretation of data: X.-F Yu, F. Gao, W. Li, H.-D Liu; Writing, review, and/or revision of the manuscript: X.-F Yu, F. Gao, W. Li, H.-D Liu; Administrative, technical, or material support: X.-F Yu, F. Gao, W. Li, H.-D Liu; Study supervision: X.-F Yu, F. Gao, W. Li, H.-D Liu.

Acknowledgements

We would like to thank Shiming Tan at the Third Xiangya Hospital of Central South University for technical assistance.

References

1. Sung H, Ferlay J, Siegel RL, Laversanne M, Soerjomataram I, Jemal A, et al. Global Cancer Statistics 2020: GLOBOCAN Estimates of Incidence and Mortality Worldwide for 36 Cancers in 185 Countries. CA Cancer J Clin. 2021;71(3):209–49.
2. George TJ, Franke AJ, Chakravarthy AB, Das P, Dasari A, El-Rayes BF, et al. National Cancer Institute (NCI) state of the science: Targeted radiosensitizers in colorectal cancer. Cancer. 2019;125(16):2732–46.
3. Beroukhim R, Mermel CH, Porter D, Wei G, Raychaudhuri S, Donovan J, et al. The landscape of somatic copy-number alteration across human cancers. Nature. 2010;463(7283):899–905.
4. Nangia V, Siddiqui FM, Caenepeel S, Timonina D, Bilton SJ, Phan N, et al. Exploiting MCL1 Dependency with Combination MEK + MCL1 Inhibitors Leads to Induction of Apoptosis and Tumor Regression in KRAS-Mutant Non-Small Cell Lung Cancer. Cancer Discov. 2018;8(12):1598–613.
5. Greaves G, Milani M, Butterworth M, Carter RJ, Byrne DP, Eyers PA, et al. BH3-only proteins are dispensable for apoptosis induced by pharmacological inhibition of both MCL-1 and BCL-XL. Cell Death Differ. 2019;26(6):1037–47.
6. Song P, Yang S, Hua H, Zhang H, Kong Q, Wang J, et al. The regulatory protein GADD34 inhibits TRAIL-induced apoptosis via TRAF6/ERK-dependent stabilization of myeloid cell leukemia 1 in liver cancer cells. J Biol Chem. 2019;294(15):5945–55.
7. Pradhan AK, Bhoopathi P, Talukdar S, Shen XN, Emdad L, Das SK, et al. Recombinant MDA-7/IL24 Suppresses Prostate Cancer Bone Metastasis through Downregulation of the Akt/Mcl-1 Pathway. Mol Cancer Ther. 2018;17(9):1951–60.
8. Siu KT, Huang C, Panaroni C, Mukaihara K, Fulzele K, Soucy R, et al. BCL2 blockade overcomes MCL1 resistance in multiple myeloma. Leukemia. 2019;33(8):2098–102.
9. Kelly PN, Strasser A. The role of Bcl-2 and its pro-survival relatives in tumourigenesis and cancer therapy. Cell Death Differ. 2011;18(9):1414–24.
10. Perciavalle RM, Opferman JT. Delving deeper: MCL-1's contributions to normal and cancer biology. Trends Cell Biol. 2013;23(1):22–9.
11. Zhang H, Guttikonda S, Roberts L, Uziel T, Semizarov D, Elmore SW, et al. Mcl-1 is critical for survival in a subgroup of non-small-cell lung cancer cell lines. Oncogene. 2011;30(16):1963–8.
12. Feng C, Yang F, Wang J. FBXO4 inhibits lung cancer cell survival by targeting Mcl-1 for degradation. Cancer Gene Ther. 2017;24(8):342–7.
13. Gao F, Yu X, Li M, Zhou L, Liu W, Li W, et al. Deguelin suppresses non-small cell lung cancer by inhibiting EGFR signaling and promoting GSK3beta/FBW7-mediated Mcl-1 destabilization. Cell Death Dis. 2020;11(2):143.
14. Wang R, Xia L, Gabrilove J, Waxman S, Jing Y. Sorafenib Inhibition of Mcl-1 Accelerates ATRA-Induced Apoptosis in Differentiation-Responsive AML Cells. Clin Cancer Res. 2016;22(5):1211–21.
15. Allan LA, Skowyra A, Rogers KI, Zeller D, Clarke PR. Atypical APC/C-dependent degradation of Mcl-1 provides an apoptotic timer during mitotic arrest. EMBO J. 2018;37:17.

16. Yu X, Wang R, Zhang Y, Zhou L, Wang W, Liu H, et al. Skp2-mediated ubiquitination and mitochondrial localization of Akt drive tumor growth and chemoresistance to cisplatin. Oncogene. 2019;38(50):7457–72.
17. Zhou L, Yu X, Li M, Gong G, Liu W, Li T, et al. Cdh1-mediated Skp2 degradation by dioscin reprogrammes aerobic glycolysis and inhibits colorectal cancer cells growth. EBioMedicine. 2020;51:102570.
18. Liu H, Liu K, Huang Z, Park CM, Thimmegowda NR, Jang JH, et al. A chrysin derivative suppresses skin cancer growth by inhibiting cyclin-dependent kinases. J Biol Chem. 2013;288(36):25924–37.
19. Liu W, Li W, Liu H, Yu X. Xanthohumol inhibits colorectal cancer cells via downregulation of Hexokinases II-mediated glycolysis. Int J Biol Sci. 2019;15(11):2497–508.
20. Inuzuka H, Shaik S, Onoyama I, Gao D, Tseng A, Maser RS, et al. SCF(FBW7) regulates cellular apoptosis by targeting MCL1 for ubiquitylation and destruction. Nature. 2011;471(7336):104–9.
21. Zhong Q, Gao W, Du F, Wang X. Mule/ARF-BP1, a BH3-only E3 ubiquitin ligase, catalyzes the polyubiquitination of Mcl-1 and regulates apoptosis. Cell. 2005;121(7):1085–95.
22. Ding Q, He X, Hsu JM, Xia W, Chen CT, Li LY, et al. Degradation of Mcl-1 by beta-TrCP mediates glycogen synthase kinase 3-induced tumor suppression and chemosensitization. Mol Cell Biol. 2007;27(11):4006–17.
23. Wertz IE, Kusam S, Lam C, Okamoto T, Sandoval W, Anderson DJ, et al. Sensitivity to antitubulin chemotherapeutics is regulated by MCL1 and FBW7. Nature. 2011;471(7336):110–4.
24. Sarraf SA, Raman M, Guarani-Pereira V, Sowa ME, Huttlin EL, Gygi SP, et al. Landscape of the PARKIN-dependent ubiquitylome in response to mitochondrial depolarization. Nature. 2013;496(7445):372–6.
25. Carroll RG, Hollville E, Martin SJ. Parkin sensitizes toward apoptosis induced by mitochondrial depolarization through promoting degradation of Mcl-1. Cell Rep. 2014;9(4):1538–53.
26. Magiera MM, Mora S, Mojsa B, Robbins I, Lassot I, Desagher S. Trim17-mediated ubiquitination and degradation of Mcl-1 initiate apoptosis in neurons. Cell Death Differ. 2013;20(2):281–92.
27. Harley ME, Allan LA, Sanderson HS, Clarke PR. Phosphorylation of Mcl-1 by CDK1-cyclin B1 initiates its Cdc20-dependent destruction during mitotic arrest. EMBO J. 2010;29(14):2407–20.
28. Choi YB, Harhaj EW. HTLV-1 tax stabilizes MCL-1 via TRAF6-dependent K63-linked polyubiquitination to promote cell survival and transformation. PLoS Pathog. 2014;10(10):e1004458.
29. Schwickart M, Huang X, Lill JR, Liu J, Ferrando R, French DM, et al. Deubiquitinase USP9X stabilizes MCL1 and promotes tumour cell survival. Nature. 2010;463(7277):103–7.
30. Wang B, Xie M, Li R, Owonikoko TK, Ramalingam SS, Khuri FR, et al. Role of Ku70 in deubiquitination of Mcl-1 and suppression of apoptosis. Cell Death Differ. 2014;21(7):1160–9.
31. Wu X, Luo Q, Zhao P, Chang W, Wang Y, Shu T, et al. JOSD1 inhibits mitochondrial apoptotic signalling to drive acquired chemoresistance in gynaecological cancer by stabilizing MCL1. Cell Death Differ. 2020;27(1):55–70.

32. Wu X, Luo Q, Zhao P, Chang W, Wang Y, Shu T, et al. MGMT-activated DUB3 stabilizes MCL1 and drives chemoresistance in ovarian cancer. Proc Natl Acad Sci U S A. 2019;116(8):2961–6.
33. Zhang S, Zhang M, Jing Y, Yin X, Ma P, Zhang Z, et al. Deubiquitinase USP13 dictates MCL1 stability and sensitivity to BH3 mimetic inhibitors. Nat Commun. 2018;9(1):215.
34. Frescas D, Pagano M. Deregulated proteolysis by the F-box proteins SKP2 and beta-TrCP: tipping the scales of cancer. Nat Rev Cancer. 2008;8(6):438–49.
35. Yu ZK, Gervais JL, Zhang H. Human CUL-1 associates with the SKP1/SKP2 complex and regulates p21(CIP1/WAF1) and cyclin D proteins. Proc Natl Acad Sci U S A. 1998;95(19):11324–9.
36. Tsvetkov LM, Yeh KH, Lee SJ, Sun H, Zhang H. p27(Kip1) ubiquitination and degradation is regulated by the SCF(Skp2) complex through phosphorylated Thr187 in p27. Curr Biol. 1999;9(12):661–4.
37. Kamura T, Hara T, Kotoshiba S, Yada M, Ishida N, Imaki H, et al. Degradation of p57Kip2 mediated by SCFSkp2-dependent ubiquitylation. Proc Natl Acad Sci U S A. 2003;100(18):10231–6.
38. Inuzuka H, Gao D, Finley LW, Yang W, Wan L, Fukushima H, et al. Acetylation-dependent regulation of Skp2 function. Cell. 2012;150(1):179–93.
39. Huang H, Regan KM, Wang F, Wang D, Smith DI, van Deursen JM, et al. Skp2 inhibits FOXO1 in tumor suppression through ubiquitin-mediated degradation. Proc Natl Acad Sci U S A. 2005;102(5):1649–54.
40. Chan CH, Li CF, Yang WL, Gao Y, Lee SW, Feng Z, et al. The Skp2-SCF E3 ligase regulates Akt ubiquitination, glycolysis, herceptin sensitivity, and tumorigenesis. Cell. 2012;149(5):1098–111.
41. Wang Z, Gao D, Fukushima H, Inuzuka H, Liu P, Wan L, et al. Skp2: a novel potential therapeutic target for prostate cancer. Biochim Biophys Acta. 2012;1825(1):11–7.
42. Wang Z, Liu P, Inuzuka H, Wei W. Roles of F-box proteins in cancer. Nat Rev Cancer. 2014;14(4):233–47.
43. Shapira M, Ben-Izhak O, Linn S, Futerman B, Minkov I, Hershko DD. The prognostic impact of the ubiquitin ligase subunits Skp2 and Cks1 in colorectal carcinoma. Cancer. 2005;103(7):1336–46.
44. Vasile Bochis O, Achimas-Cadariu P, Vlad C, Fetica B, Corneliu Leucuta D, Ioan Busuioc C, et al. The prognostic role of Skp2 and the tumor suppressor protein p27 in colorectal cancer. J BUON. 2017;22(5):1122–30.
45. Totary-Jain H, Sanoudou D, Dautriche CN, Schneller H, Zambrana L, Marks AR. Rapamycin resistance is linked to defective regulation of Skp2. Cancer Res. 2012;72(7):1836–43.
46. Davidovich S, Ben-Izhak O, Shapira M, Futerman B, Hershko DD. Over-expression of Skp2 is associated with resistance to preoperative doxorubicin-based chemotherapy in primary breast cancer. Breast Cancer Res. 2008;10(4):R63.
47. Yang Q, Huang J, Wu Q, Cai Y, Zhu L, Lu X, et al. Acquisition of epithelial-mesenchymal transition is associated with Skp2 expression in paclitaxel-resistant breast cancer cells. Br J Cancer. 2014;110(8):1958–67.

48. Wang XC, Tian LL, Tian J, Jiang XY. Overexpression of SKP2 promotes the radiation resistance of esophageal squamous cell carcinoma. Radiat Res. 2012;177(1):52–8.
49. Akhoondi S, Lindstrom L, Widschwendter M, Corcoran M, Bergh J, Spruck C, et al. Inactivation of FBXW7/hCDC4-beta expression by promoter hypermethylation is associated with favorable prognosis in primary breast cancer. Breast Cancer Res. 2010;12(6):R105.
50. O'Neil J, Look AT. Mechanisms of transcription factor deregulation in lymphoid cell transformation. Oncogene. 2007;26(47):6838–49.
51. Davis RJ, Welcker M, Clurman BE. Tumor suppression by the Fbw7 ubiquitin ligase: mechanisms and opportunities. Cancer Cell. 2014;26(4):455–64.
52. Wang Z, Fukushima H, Gao D, Inuzuka H, Wan L, Lau AW, et al. The two faces of FBW7 in cancer drug resistance. Bioessays. 2011;33(11):851–9.
53. Iwatsuki M, Mimori K, Ishii H, Yokobori T, Takatsuno Y, Sato T, et al. Loss of FBXW7, a cell cycle regulating gene, in colorectal cancer: clinical significance. Int J Cancer. 2010;126(8):1828–37.
54. Yeh CH, Bellon M, Nicot C. FBXW7: a critical tumor suppressor of human cancers. Mol Cancer. 2018;17(1):115.
55. King B, Trimarchi T, Reavie L, Xu L, Mullenders J, Ntziachristos P, et al. The ubiquitin ligase FBXW7 modulates leukemia-initiating cell activity by regulating MYC stability. Cell. 2013;153(7):1552–66.
56. Koepp DM, Schaefer LK, Ye X, Keyomarsi K, Chu C, Harper JW, et al. Phosphorylation-dependent ubiquitination of cyclin E by the SCFFbw7 ubiquitin ligase. Science. 2001;294(5540):173–7.
57. Nateri AS, Riera-Sans L, Da Costa C, Behrens A. The ubiquitin ligase SCFFbw7 antagonizes apoptotic JNK signaling. Science. 2004;303(5662):1374–8.
58. Onoyama I, Suzuki A, Matsumoto A, Tomita K, Katagiri H, Oike Y, et al. Fbxw7 regulates lipid metabolism and cell fate decisions in the mouse liver. J Clin Invest. 2011;121(1):342–54.
59. Khan OM, Carvalho J, Spencer-Dene B, Mitter R, Frith D, Snijders AP, et al. The deubiquitinase USP9X regulates FBW7 stability and suppresses colorectal cancer. J Clin Invest. 2018;128(4):1326–37.
60. Khan OM, Almagro J, Nelson JK, Horswell S, Encheva V, Keyan KS, et al. Proteasomal degradation of the tumour suppressor FBW7 requires branched ubiquitylation by TRIP12. Nat Commun. 2021;12(1):2043.
61. Miyachi M, Kakazu N, Yagyu S, Katsumi Y, Tsubai-Shimizu S, Kikuchi K, et al. Restoration of p53 pathway by nutlin-3 induces cell cycle arrest and apoptosis in human rhabdomyosarcoma cells. Clin Cancer Res. 2009;15(12):4077–84.
62. Shen H, Zhang J, Wang C, Jain PP, Xiong M, Shi X, et al. MDM2-Mediated Ubiquitination of Angiotensin-Converting Enzyme 2 Contributes to the Development of Pulmonary Arterial Hypertension. Circulation. 2020;142(12):1190–204.
63. Song C, Lowe VJ, Lee S. Inhibition of Cdc20 suppresses the metastasis in triple negative breast cancer (TNBC). Breast Cancer. 2021. doi:10.1007/s12282-021-01242-z.

64. Chan CH, Morrow JK, Li CF, Gao Y, Jin G, Moten A, et al. Pharmacological inactivation of Skp2 SCF ubiquitin ligase restricts cancer stem cell traits and cancer progression. Cell. 2013;154(3):556–68.
65. Zhang F, Xia X, Chai R, Xu R, Xu Q, Liu M, et al. Inhibition of USP14 suppresses the formation of foam cell by promoting CD36 degradation. J Cell Mol Med. 2020;24(6):3292–302.
66. Liu J, Xia H, Kim M, Xu L, Li Y, Zhang L, et al. Beclin1 controls the levels of p53 by regulating the deubiquitination activity of USP10 and USP13. Cell. 2011;147(1):223–34.
67. Weinstock J, Wu J, Cao P, Kingsbury WD, McDermott JL, Kodrasov MP, et al. Selective Dual Inhibitors of the Cancer-Related Deubiquitylating Proteases USP7 and USP47. ACS Med Chem Lett. 2012;3(10):789–92.
68. Lei H, Xu HZ, Shan HZ, Liu M, Lu Y, Fang ZX, et al. Targeting USP47 overcomes tyrosine kinase inhibitor resistance and eradicates leukemia stem/progenitor cells in chronic myelogenous leukemia. Nat Commun. 2021;12(1):51.
69. Sun H, Kapuria V, Peterson LF, Fang D, Bornmann WG, Bartholomeusz G, et al. Bcr-Abl ubiquitination and Usp9x inhibition block kinase signaling and promote CML cell apoptosis. Blood. 2011;117(11):3151–62.

Figures

Figure 1

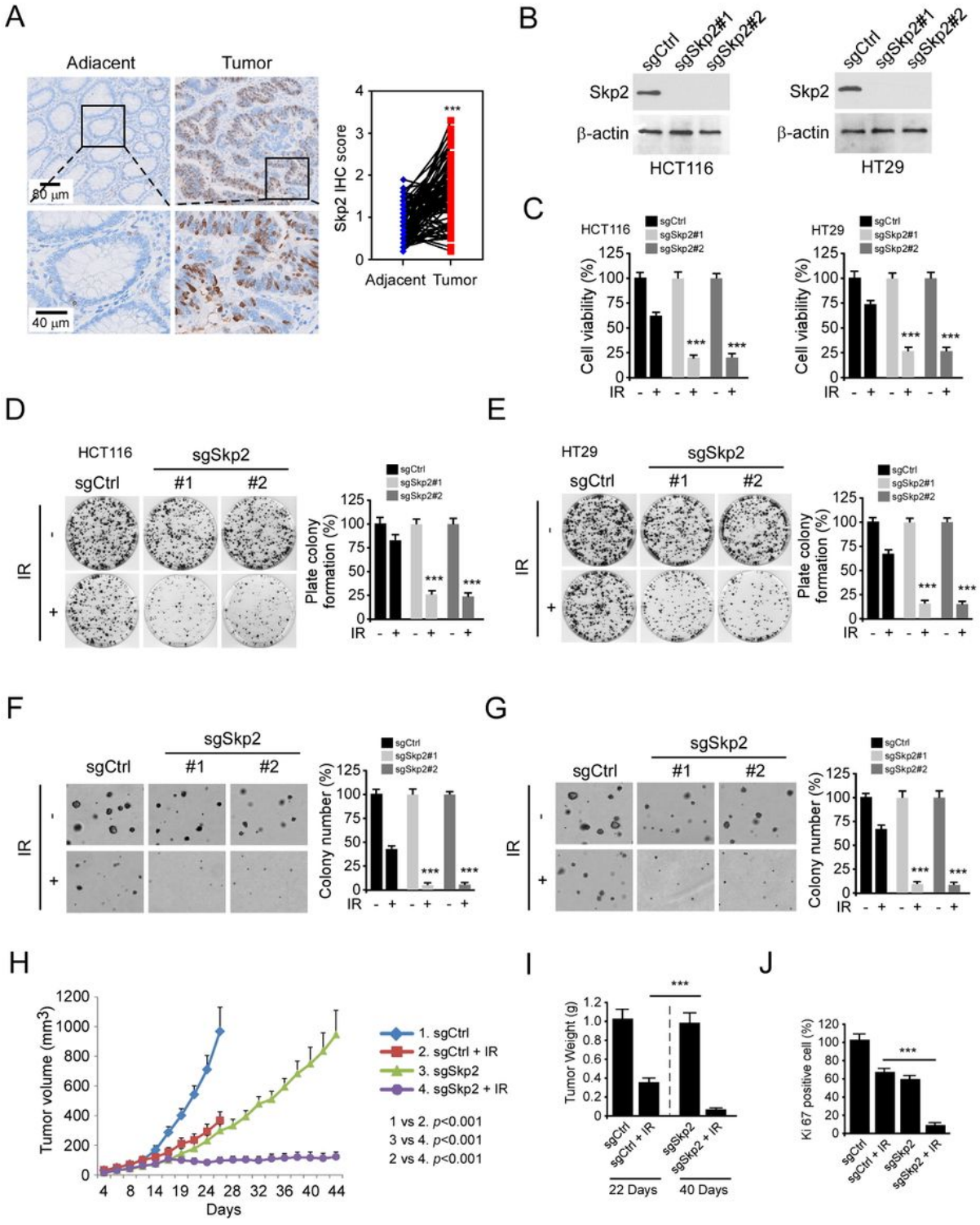

Figure 1

Skp2 is required for the maintaining of tumorigenic properties of human colorectal cancer (CRC) cells. A, left, the representative staining images of CRC specimens and adjacent tissues; right, quantification of the staining intensity using Image-Pro PLUS (v.6) and Image J (NIH) computer software. ***p<0.001. a significant difference between groups as indicated. B, immunoblot (IB) analysis of Skp2 protein level in Skp2 knock out CRC stable cell lines. C, MTS assay was performed to determine the cell viability of Skp2

knock out CRC stable cell lines treated with/without 2Gy irradiation (IR). ***p<0.001. D and E, plate colony formation assay analysis of the colony formation of Skp2 knock out HCT116 (D) and HT29 (E) stable cell lines treated with/without IR (2Gy). ***p<0.001. F and G, soft agar assay determination of the anchorage-independent cell growth of Skp2 knock out HCT116 (F) and HT29 (G) stable cell lines treated with/without IR (2Gy). ***p<0.001. H-J, average tumor volume (H), average tumor weight (I), and the population of Ki67 positive cells of HCT116-sgCtrl and HCT116-sgSkp2 xenografts treated with/without IR. ***p<0.001.

Figure 2

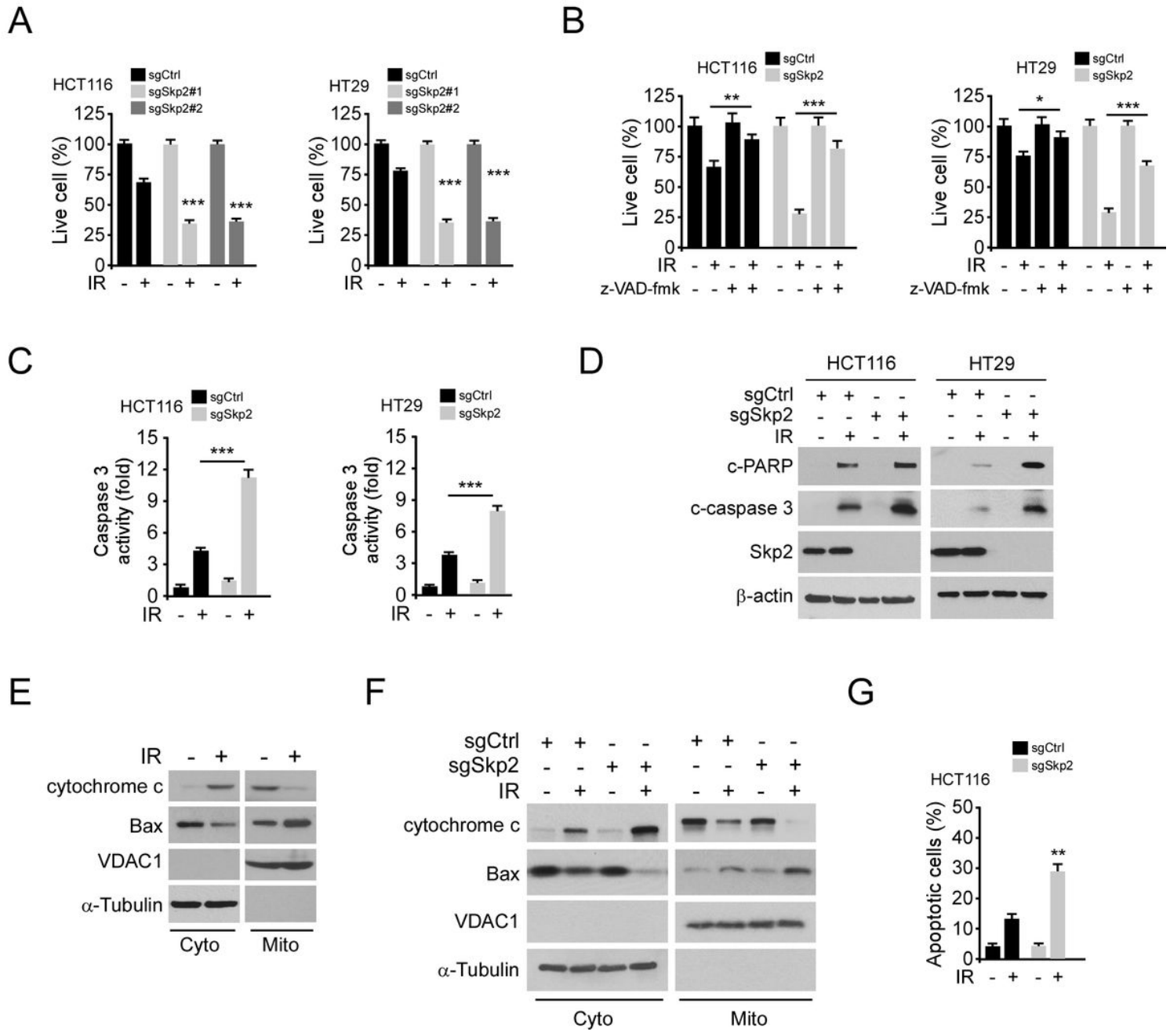

Figure 2

Depletion of Skp2 enhances IR-induced intrinsic apoptosis. A, Skp2 knockout CRC stable cells were treated with/without IR (2Gy) and cultured for 72 h, live cell population was determined by trypan blue exclusion assay. ***p<0.001. B and C, Skp2 knockout CRC stable cells were pretreated with pan-caspase inhibitor z-VAD-fmk for 4 h, followed by 2Gy IR treatment. Cells were cultured for 72 h, live cell population was determined by trypan blue exclusion assay (B), caspase 3 activity was examined by Caspase 3 Assay Kit (C). *p<0.05, **p<0.01, ***p<0.001. D, Skp2 knockout HCT116 (left) and HT29 (right) stable cells were treated with/without IR (2Gy) and cultured for 72 h, whole-cell extract (WCE) was subjected to IB analysis. E, HCT116 cells were treated with/without IR (2Gy) and cultured for 72 h, subcellular fractions were isolated and subjected to IB analysis. F and G, Skp2 knockout HCT116 stable cells were treated with/without IR (2Gy) and cultured for 72 h, subcellular factions were isolated and subjected to IB analysis (F), the population of apoptotic cells was examined by flow cytometry (G). **p<0.01.

Figure 3

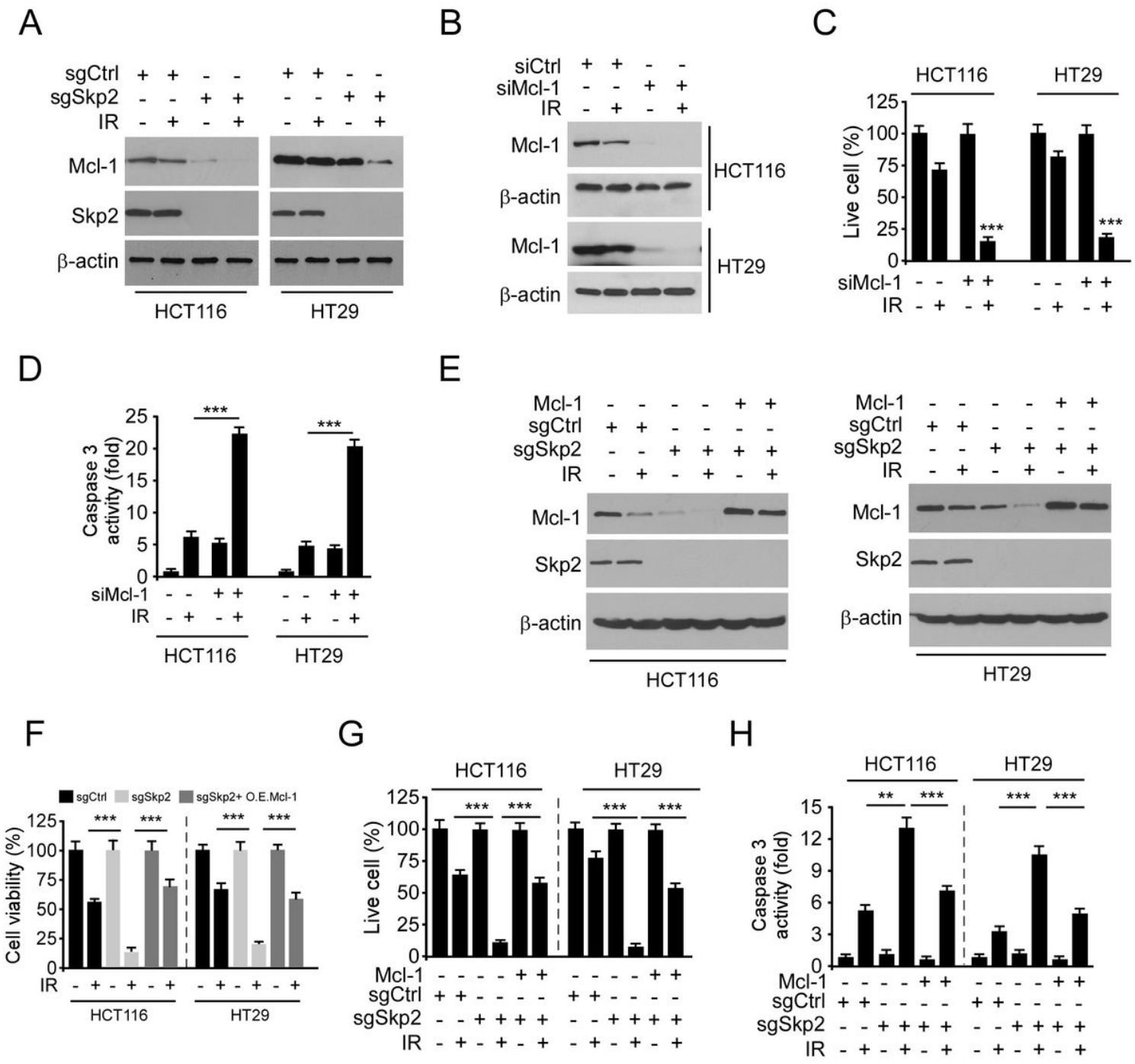

Figure 3

Irradiation decreases Mcl-1 protein level. A, Skp2 knockout CRC stable cells were treated with/without IR (2Gy) and cultured for 72 h, WCE were subjected to IB analysis. B-D, HCT116 and HT29 cells were transfected with siMcl-1 for 24 h, followed by IR (2Gy) treated and cultured for 72 h. WCE were subjected to IB analysis (B). Live cell population was determined by trypan blue exclusion assay (C). Caspase 3 activity was examined by Caspase 3 Assay Kit (D). ***p<0.001. E-H, Mcl-1 was transient transfected into Skp2 depleted HCT116 and HT29 cells, followed by IR (2Gy) treated and cultured for 72 h. WCE were

subjected to IB analysis (E). Cell viability and Live cell population was determined by MTS assay (F) and trypan blue exclusion assay (G), respectively. Caspase 3 activity was examined by Caspase 3 Assay Kit (H). **p<0.01, ***p<0.001.

Figure 4

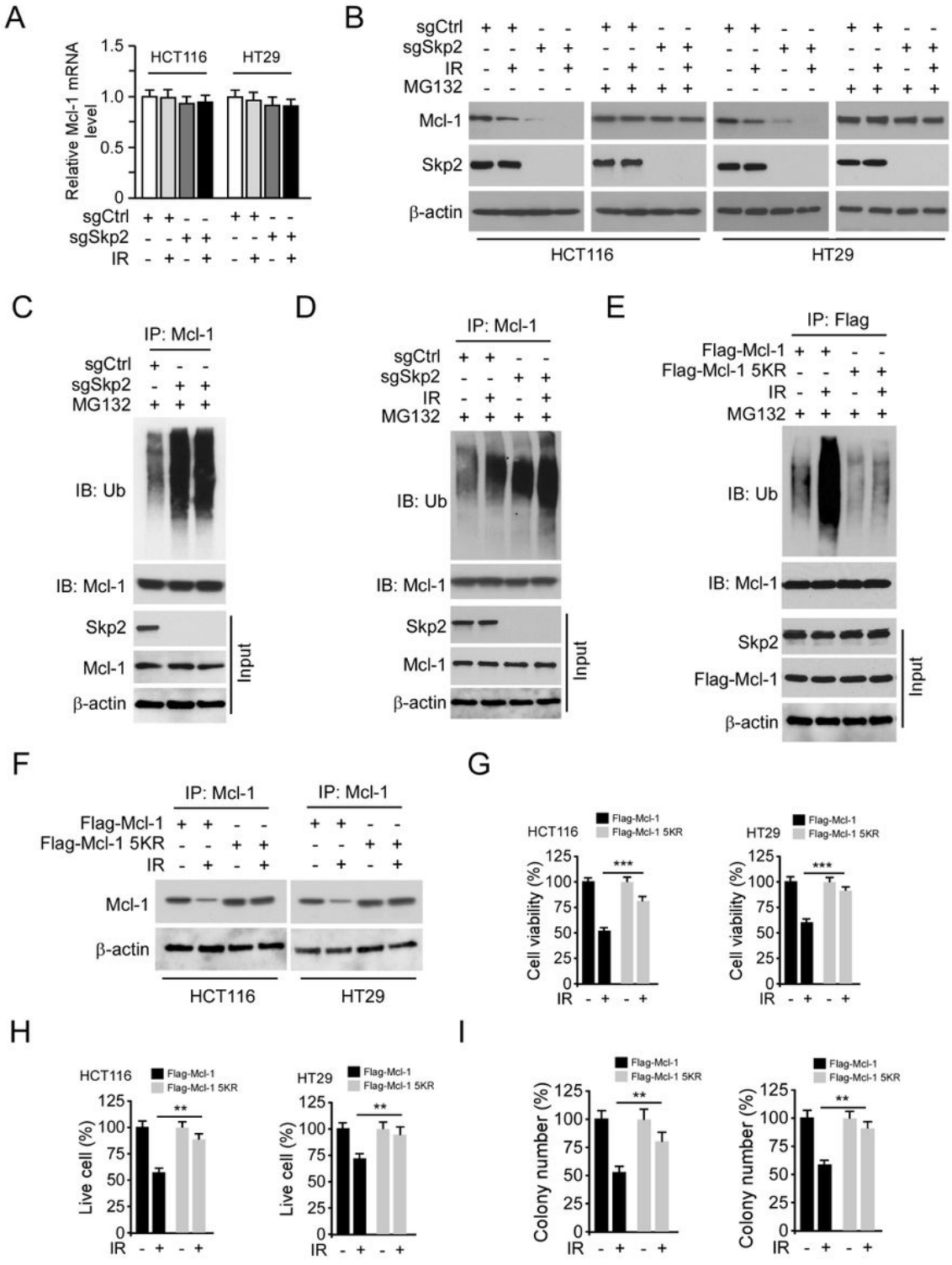

Figure 4

Irradiation promotes Mcl-1 ubiquitination and degradation. A, Mcl-1 mRNA expression in Skp2 depleted CRC cells with IR treatment was examined by real-time RT-PCR. B, Skp2 depleted HCT116 and HT29 cells

were treated with IR (2Gy) and cultured for 72 h, MG132 (25 μm) was added to cell culture medium and maintained for 6 h. WCE was subjected to IB analysis. C, Skp2 knockout HCT116 cells were treated with MG132 for 6 h, WCE was prepared and subjected to Mcl-1 ubiquitination analysis. D, Skp2 depleted HCT116 cells were treated with MG132 (25 μM) for 6 h, followed by IR (2Gy) treatment and cultured for 1 h. WCE was subjected to Mcl-1 ubiquitination analysis. E, Flag-Mcl-1 wild type or 5KR mutant was transfected into HCT116 cells for 48 h and treated with IR. WCE was extracted after IR treatment for 1 h and subjected to Mcl-1 ubiquitination analysis. F, Flag-Mcl-1 wild type or 5KR mutant was transfected into HCT116 cells for 24 h, followed by IR (2Gy) treatment and cultured for 72 h. WCE was subjected to IB analysis. G-I, Flag-Mcl-1 wild type or 5KR mutant was transfected into HCT116 cells for 24 h, followed by IR (2Gy) treatment and cultured for 72 h. Cell viability and Live cell population was determined by MTS assay (G) and trypan blue exclusion assay (H), respectively. Colony formation was examined by plate colony formation assay (I). **p<0.01, ***p<0.001.

Figure 5

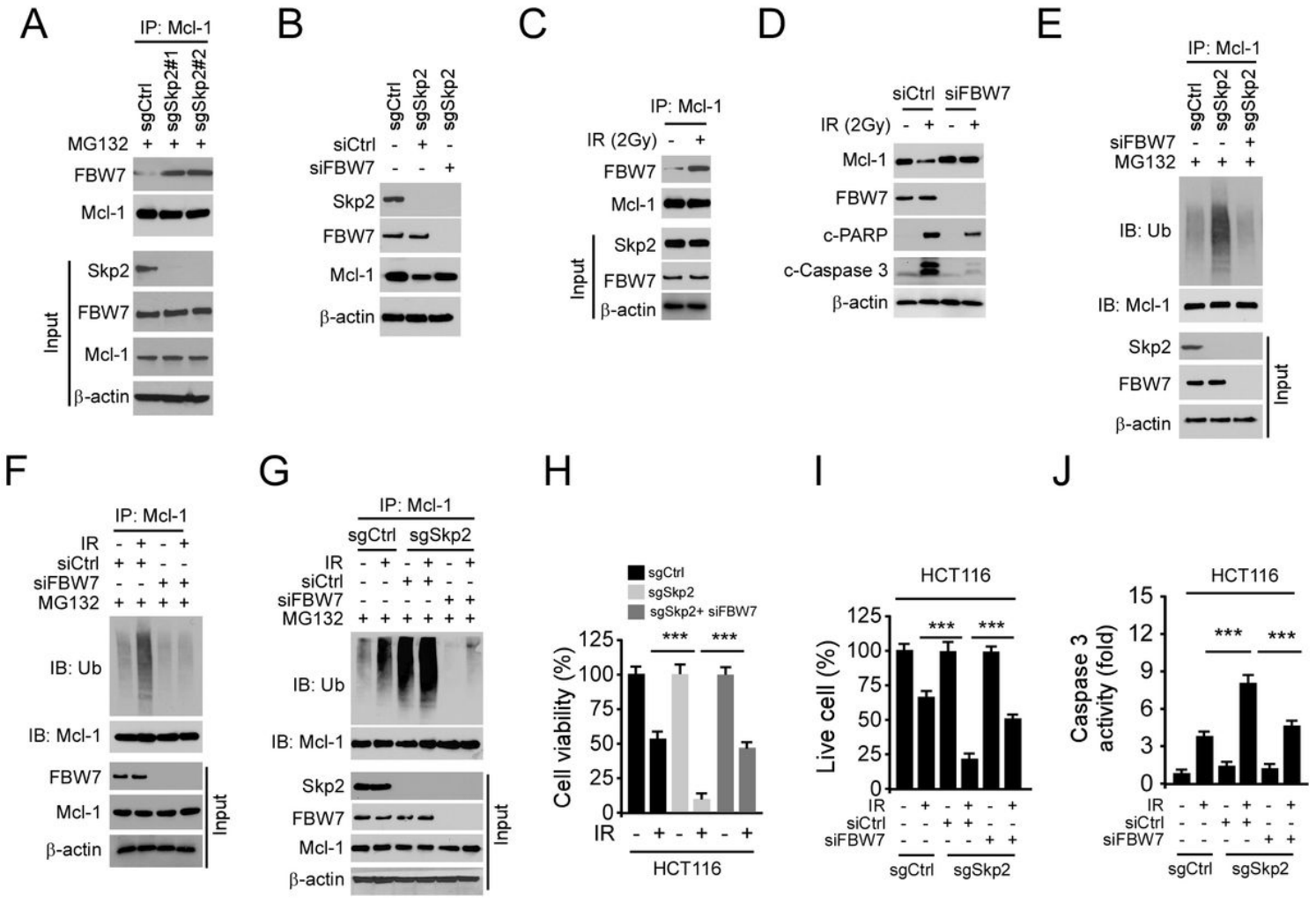

Figure 5

FBW7 is required for IR-induced Mcl-1 ubiquitination. A, Skp2 knockout HCT116 cells were treated with MG132 for 6 h, WCE was subjected to co-immunoprecipitation (Co-IP) analysis. B, siFBW7 was

transfected into Skp2 depleted HCT116 cells and subjected to IB analysis. C, HCT116 cells were treated with IR (2Gy), WCE was collected 1 h later and subjected to Co-IP analysis. D, siFBW7 was transfected into HCT116 cells for 24 h, followed by IR (2Gy) treatment. Cells were cultured for 72 h, WCE was subjected to IB analysis. E, siFBW7 was transfected into Skp2 depleted HCT116 cells for 48 h, followed by MG132 treatment for 6 h, WCE was subjected to Mcl-1 ubiquitination analysis. F, HCT116 cells were transfected with siCtrl or siFBW7 and cultured for 48 h. After incubated with MG132 for 6 h, the cells were treated with IR. WCE was collected 1 h later and subjected to Mcl-1 ubiquitination analysis. G-J, Skp2 depleted HCT116 cells were transfected with siCtrl or siFBW7 and cultured for 48 h. After incubated with MG132 for 6 h, the cells were treated with IR. WCE was collected 1 h later and subjected to Mcl-1 ubiquitination analysis (G). Cell viability and Live cell population was determined by MTS assay (H) and trypan blue exclusion assay (I), respectively. Caspase 3 activity was examined by Caspase 3 Assay Kit (J). ***$p<0.001$.

Figure 6

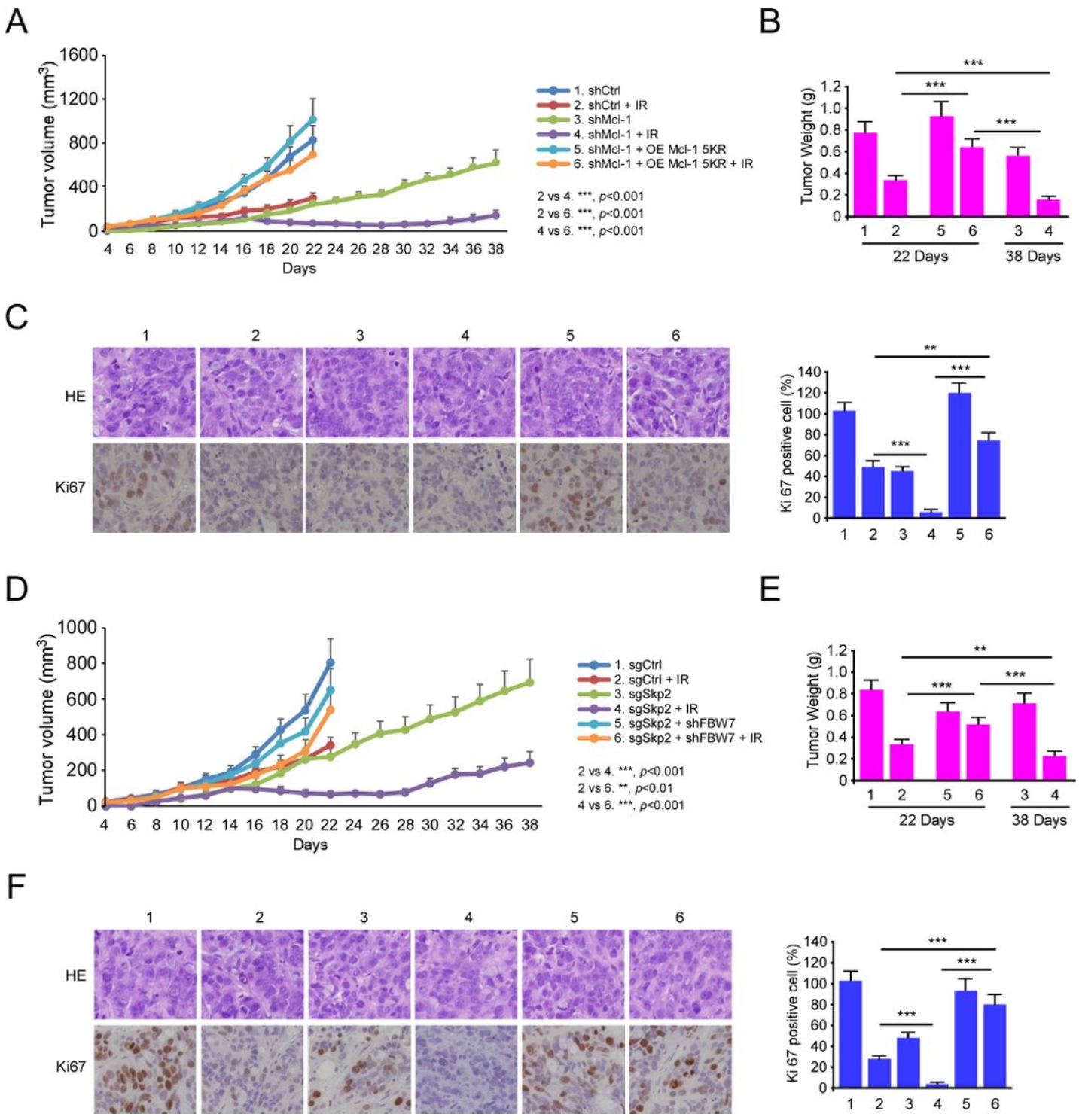

Figure 6

Irradiation inhibits in vivo tumor growth. A-C, Mcl-1 5KR reintroduction into Mcl-1 knockdown HCT116 cells rescues tumorigenesis under IR treatment. Mcl-1 5KR mutant was reintroduced into Mcl-1 knockdown HCT116 cells and injected into nude mice to establish the xenograft mouse model. Tumor size was monitored (A). Tumors were weighed (B). Ki67 positive cells were examined by IHC staining (C). **p<0.01, ***p<0.001. D-F, Knockdown of FBW7 into Skp2-null HCT116 cells rescues tumorigenesis under

IR treatment. FBW7 was silenced in Skp2-null HCT116 cells and injected into nude mice to establish the xenograft mouse model. Tumor size was monitored (D). Tumors were weighed (E). Ki67 positive cells were examined by IHC staining (F). **p<0.01, ***p<0.001.

Figure 7

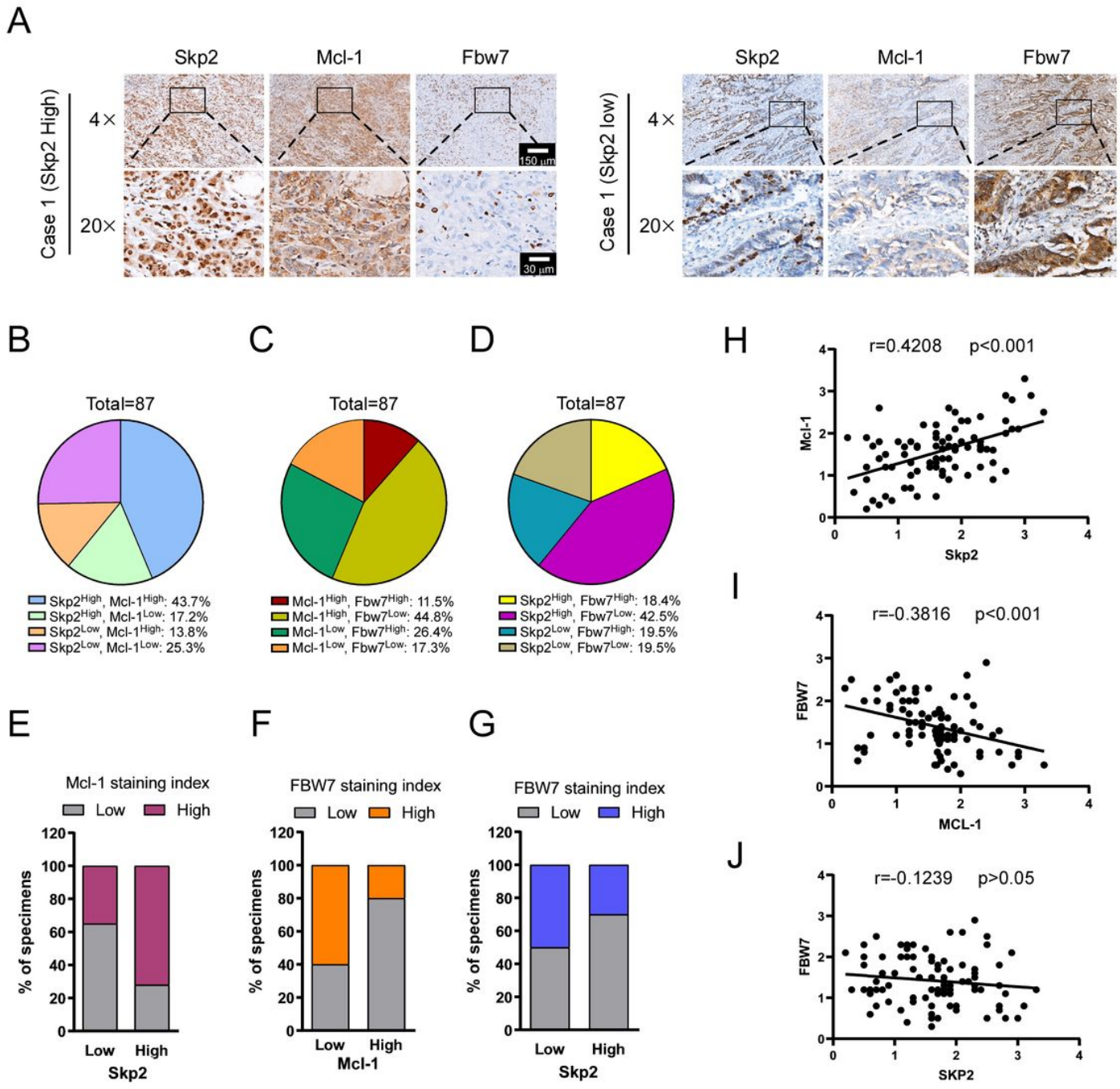

Figure 7

Skp2 positively correlates with Mcl-1 in CRC tissues. A, representative cases from 87 CRC specimens were analyzed by IHC staining with Skp2, Mcl-1, and FBW7. B-D, the expression of Skp2 and Mcl-1 (B), Mcl-1 and Fbw7 (C), and Skp2 and FBW7 (D) in 87 CRC specimens were analyzed. The relative proportions of protein expressions were illustrated as a pie chart. E, the percentage of samples displaying low or high

Skp2 expression compared to the expression levels of Mcl-1. F, the percentage of specimens displaying low or high Mcl-1 expression compared to the expression levels of FBW7. G, the percentage of specimens displaying low or high Skp2 expression compared to the expression levels of FBW7. H, scatterplot showing the positive correlation between Skp2 and Mcl-1. I, scatterplot showing the negative correlation between Mcl-1 and FBW7. J, scatterplot showing no correlation between Skp2 and FBW7.

Supplementary Files

This is a list of supplementary files associated with this preprint. Click to download.

- FigureS1.jpg
- FigureS2.jpg
- SupplementaryFigurelegend20210621.doc
- SupplementaryTable120210621.docx
- SupplementaryTable220210621.docx